

Myeloid Cell mPges-1 Deletion Attenuates Mortality Without Affecting Remodeling After Acute Myocardial Infarction in Mice

Lihong Chen,¹ Guangrui Yang,¹ Tingting Jiang,¹ Soon Yew Tang, Tao Wang, Qing Wan, Miao Wang, and Garret A. FitzGerald

Advanced Institute for Medical Sciences, Dalian Medical University, Dalian, China (L.C., T.J.); School of Life Science and Biotechnology, Dalian University of Technology, Dalian, China (G.Y.); Institute for Translational Medicine and Therapeutics (L.C., G.Y., S.Y.T., G.A.F.) and Cardiovascular Institute (T.W., G.A.F.), University of Pennsylvania, Philadelphia, Pennsylvania; and State Key Laboratory of Medical Molecular Biology, Chinese Academy of Medical Sciences and Peking Union Medical College, Beijing, China (Q.W., M.W.)

Received January 3, 2019; accepted April 10, 2019

ABSTRACT

Selective deletion of microsomal prostaglandin E₂ synthase-1 (mPges-1) in myeloid cells retards atherogenesis and suppresses the vascular proliferative response to injury, while it does not predispose to thrombogenesis or hypertension. However, studies using bone marrow transplants from irradiated mice suggest that myeloid cell mPGES-1 facilitates cardiac remodeling and prolongs survival after experimental myocardial infarction (MI). Here, we addressed this question using mice lacking mPges-1 in myeloid cells, particularly macrophages [Mac-mPges-1-knockout (KO)], generated by crossing mPges-1 floxed mice with LysMCre mice and subjecting them to coronary artery ligation. Cardiac structure and function were assessed by morphometric analysis, echocardiography, and invasive hemodynamics 3, 7, and 28 days after MI. Despite a similar infarct size, in contrast to the

prior report, the post-MI survival rate was markedly improved in the Mac-mPges-1-KO mice compared with wild-type controls. Left ventricular systolic (reflected by ejection fraction, fractional shortness end systolic volume, and +dP/dt) and diastolic function (reflected by end diastolic volume, -dP/dt, and Tau), cardiac hypertrophy (reflected by left ventricular dimensions), and staining for fibrosis did not differ between the groups. In conclusion, we found that Cre-loxP-mediated deletion of mPges-1 in myeloid cells has favorable effects on post-MI survival, with no detectable adverse influence on post-MI remodeling. These results add to evidence that targeting macrophage mPGES-1 may represent a safe and efficacious approach to the treatment and prevention of cardiovascular inflammatory disease.

Introduction

Cyclooxygenases (COX-1 and -2) convert arachidonic acid to prostanoids. The inducible COX-2 and one of its products, prostaglandin E₂ (PGE₂), dominate prostanoid production in inflammation and pain. COX-2 selective nonsteroidal anti-inflammatory drugs have been used in the management of pyrexia and alleviation of pain and inflammation (Grosser et al., 2017b). However, despite their efficacy, it has become evident that COX-2 inhibitors increase the incidence of cardiovascular adverse events, including myocardial infarction, stroke, hypertension, heart failure, and sudden cardiac death (Grosser et al., 2017a). This results from suppression of COX-2-derived cardioprotective prostanoids, particularly prostacyclin (PGI₂), that attenuate atherogenesis and the response to thrombogenic and hypertensive stimuli (Yu et al., 2012).

This work was supported by the National Institutes of Health [Grant HL117798], American Heart Association [Grant 15SDG22780013 to Dr. L.C.], and National Natural Science Foundation of China [Grants 81400750, 81670242, and 81570643]. Dr. G.A.F. is the McNeil Professor in Translational Medicine and Therapeutics and a senior advisor to Calico Laboratories.

¹L.C., G.Y., and T.J. contributed equally to this work.
<https://doi.org/10.1124/jpet.118.256057>.

Given these observations and the opioid crisis, there is considerable interest in the development of novel, nonaddictive analgesic and anti-inflammatory drugs.

Interest in the prostanoid pathway has focused on microsomal PGE₂ synthase-1 (mPGES-1), which is functionally coupled with COX-2 and dominates inflammatory PGE₂ production (Friesen and Mancini, 2008; Wang and FitzGerald, 2010). We recently reported that deletion of mPges-1 in myeloid cells recapitulates effects of global enzyme deletion in that it attenuates the vascular proliferative response to injury and mitigates high-fat diet-induced atherogenesis. By contrast, deletion of mPges-1 in vascular cells promotes the proliferative response to injury and does not affect atherogenesis (Chen et al., 2013, 2014). This prompts consideration of targeted delivery of mPGES-1 inhibitors to inflammatory macrophages (Macs) as a novel therapeutic strategy.

Here, to address concerns that macrophage mPGES-1 might contribute to healing after myocardial infarction (MI), we have used genetic approaches to reveal that, although cardiac remodeling is not profoundly altered after experimental myocardial infarction, myeloid deletion of mPges-1 improves postinfarct survival.

ABBREVIATIONS: COX, cyclooxygenase; KO, knockout; Mac, macrophage; MI, myocardial infarction; mPges-1, microsomal PGE₂ synthase-1; PGE₂, prostaglandin E₂; PGI₂, prostacyclin; WT, wild type.

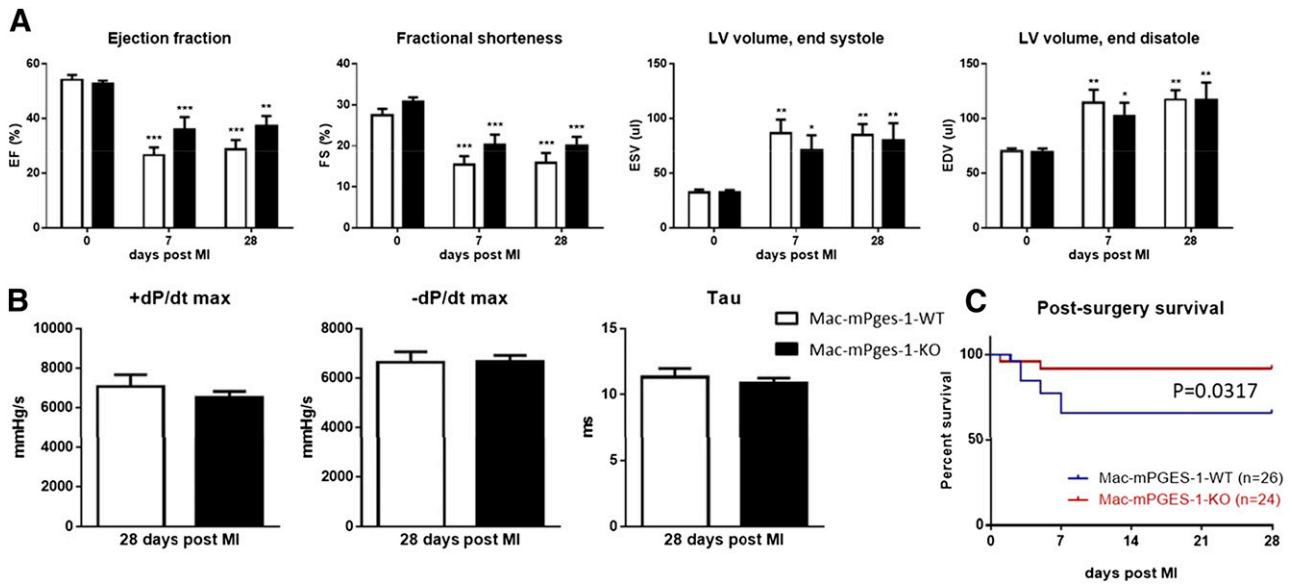


Fig. 1. Effect of myeloid mPges-1 deletion on post-MI survival and heart function. Mac-mPges-1-WT or -KO mice were subjected to coronary artery ligation and echocardiography, and hemodynamics was performed to evaluate the heart function before and 7 and 28 days after the ligation. (A) Ejection fraction (EF), fractional shortness (FS), left ventricular (LV) end-systolic volume (ESV), and end-diastolic volume (EDV). (B) The maximum ascending rate of left ventricular pressure (+dP/dt max); maximum descending rate of left ventricular pressure (-dP/dt max); left ventricular relaxation time constant (Tau); $n = 10-15$ mice/group. * $P < 0.05$; ** $P < 0.01$; *** $P < 0.001$; 0 vs. 7 or 28 days after MI. (C) Survival of Mac-mPges-1-WT and -KO mice after MI. $n = 24-26$, $P = 0.0317$, log-rank test.

Materials and Methods

Mice and the MI Model. The mPges-1 floxed mice, kindly provided by Mohammad Bohlooly of Astra Zeneca, were crossed with LysMCre mice (Jackson Laboratory, Bar Harbor, ME) to yield mice with mPges-1 deletion in myeloid cells, termed Mac-mPges-1-knockout (KO). Floxed mice in the same litters without Cre were used as controls, termed Mac-mPges-1-wild type (WT). Global mPges-1 KO and their littermate controls were obtained from Jackson Laboratory. All mice were maintained under 12-hour/12-hour light/dark conditions with free

access to food and water before and throughout experiments. Only male mice at 3 to 4 months of age were used in this study.

Mice were subjected to coronary artery ligation to induce MI as previously reported (Gao et al., 2010). In brief, after anesthetization, a skin incision was made over the left chest, and the pectoral muscles were retracted to expose the fourth intercostal space. A small hole was then made at the fourth intercostal space with a mosquito clamp to open the pleural membrane and pericardium. The heart was then carefully exteriorized. The left main descending coronary artery was

TABLE 1

Echocardiographic and hemodynamic analysis of cardiac function in myeloid mPges-1 KO mice

	Days after Coronary Ligation					
	0 (WT $n = 13$; KO $n = 15$)		7 (WT $n = 11$; KO $n = 13$)		28 (WT $n = 10$; KO $n = 13$)	
	Mac-mPges-1-WT	Mac-mPges-1-KO	Mac-mPges-1-WT	Mac-mPges-1-KO	Mac-mPges-1-WT	Mac-mPges-1-KO
Echocardiography						
Body weight (g)	27.69 ± 0.58	27.57 ± 0.65	28.88 ± 0.84	27.75 ± 0.86	30.68 ± 0.84*	28.53 ± 0.85
LV mass (mg)	85.40 ± 2.61	82.02 ± 3020	110.25 ± 6.00**	96.97 ± 5.10	109.19 ± 4.96**	103.88 ± 6.69**
LV mass/BW (mg/g)	3.09 ± 0.08	2.97 ± 0.09	3.86 ± 0.28**	3.47 ± 0.13	3.56 ± 0.14	3.61 ± 0.19**
Heart rate (bpm)	519.15 ± 14.64	480.60 ± 16.52	526.18 ± 10.57	537.46 ± 14.25	537.80 ± 10.05**	543.62 ± 11.01**
Cardiac output (ml/min)	19.53 ± 0.87	17.73 ± 1.10	14.51 ± 0.75**	16.65 ± 1.21	17.00 ± 1.51	20.16 ± 1.00
Stroke volume (μ l)	37.50 ± 0.94	36.63 ± 1.69	27.75 ± 1.70**	31.38 ± 2.68	32.04 ± 3.21	37.00 ± 1.69
Ejection fraction (%)	54.14 ± 1.84	52.85 ± 1.05	26.59 ± 2.84***	35.84 ± 4.67***	28.81 ± 3.37***	37.14 ± 3.83**
Fractional shortness (%)	27.50 ± 1.54	30.72 ± 1.10	15.37 ± 2.15***	20.18 ± 2.58***	15.83 ± 2.45***	20.15 ± 2.05***
LV volume, end systole (μ l)	32.56 ± 2.41	32.80 ± 1.79	86.62 ± 12.48**	71.04 ± 13.61*	85.23 ± 9.74**	80.02 ± 15.82**
LV volume, end diastole (μ l)	70.06 ± 2.62	69.43 ± 3.11	114.37 ± 11.98**	102.41 ± 12.0*	117.27 ± 8.71**	117.02 ± 15.87**
LV internal diameter, end systole (mm)	2.74 ± 0.12	2.52 ± 0.09	4.03 ± 0.26***	3.43 ± 0.28*	4.16 ± 0.3***	3.65 ± 0.29**
LV internal diameter, end diastole (mm)	3.77 ± 0.10	3.63 ± 0.09	4.72 ± 0.19**	4.23 ± 0.21*	4.90 ± 0.22***	4.50 ± 0.25**
Hemodynamics						
LV end systolic pressure (mm Hg)	ND	ND	ND	ND	91.90 ± 2.95	87.36 ± 1.97
LV end diastolic pressure (mm Hg)	ND	ND	ND	ND	7.48 ± 0.97	5.10 ± 0.75
LV +dP/dt max (mm Hg/s)	ND	ND	ND	ND	7071.68 ± 563.29	6516.17 ± 308.48
LV -dP/dt max (mm Hg/s)	ND	ND	ND	ND	6634.24 ± 403.96	6665.88 ± 241.52
Tau (ms)	ND	ND	ND	ND	11.31 ± 0.63	10.84 ± 0.40

BW, body weight; LV, left ventricular; ND, not determined.

* $P < 0.05$; ** $P < 0.01$; *** $P < 0.001$; 0 vs. 7 or 28 days post-MI.

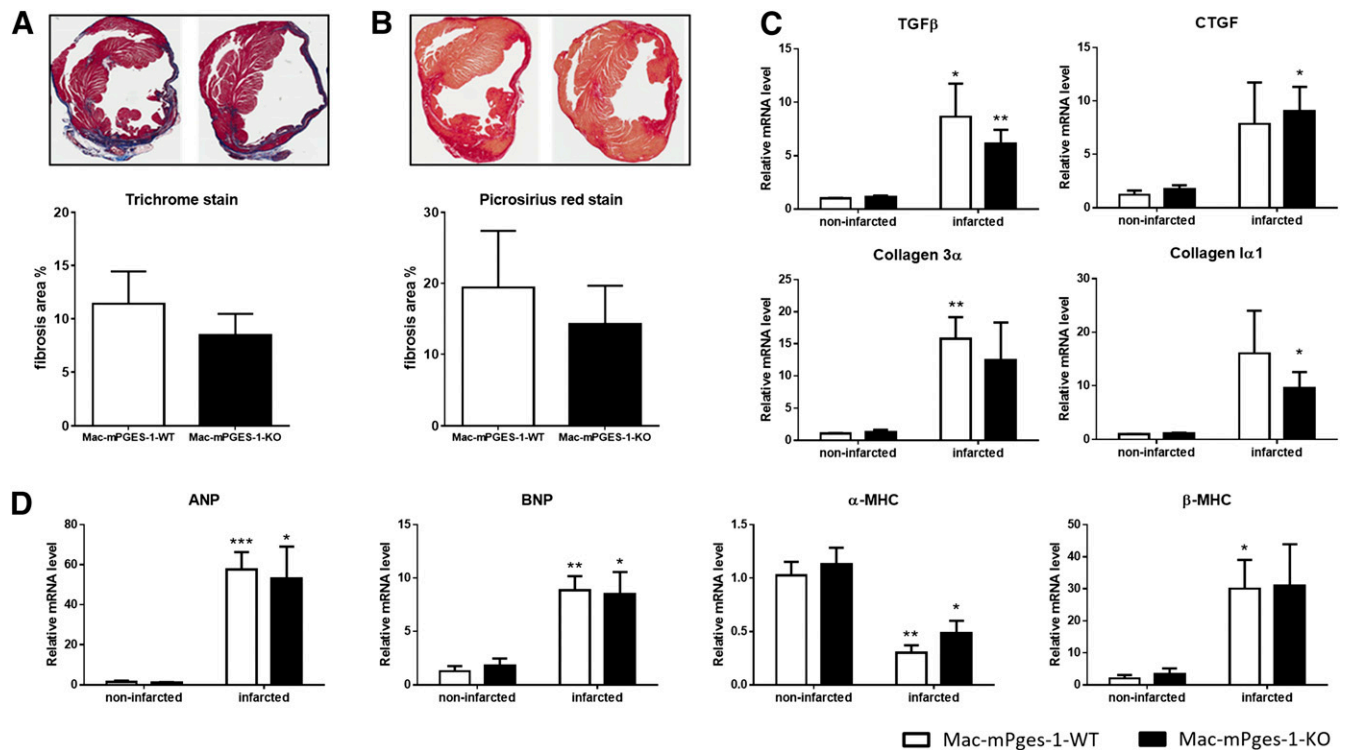


Fig. 2. Effect of myeloid mPges-1 deletion on post-MI fibrosis and hypertrophy. (A) Representative images of Masson trichrome staining and the quantitative analysis. (B) Representative images of Picrosirius red staining and the quantitative analysis. (C) Real-time polymerase chain reaction (PCR) analysis of the expression of fibrosis-related genes in the hearts from mice 28 day post-MI. (D) Real-time PCR analysis of the expression of hypertrophy-related genes in the hearts from mice 28 day post-MI. $n = 6-8$ for immunostaining; $n = 4$ to 5 for real-time PCR. * $P < 0.05$; ** $P < 0.01$; *** $P < 0.001$, noninfarcted vs. infarcted heart. ANP, atria natriuretic peptide; BNP, brain natriuretic peptide; MHC, major histocompatibility complex; TGF, transforming growth factor.

located, sutured, and ligated approximately 3 mm from its origin using a silk suture. After ligation, the heart was immediately placed back into the intrathoracic space followed by manual evacuation of air and closure of muscle and the skin. The mice were then allowed to breathe room air and monitored during the recovery period. All procedures were in accordance with the guidelines approved by the University of Pennsylvania Institutional Animal Care and Use Committee and the Animal Center at Dalian Medical University (Dalian, China).

Echocardiography and Invasive Hemodynamics. Mice were anesthetized by inhalation of 1% to 2% isoflurane via nose cone and placed on a heating pad to maintain the body temperature. Echocardiography was performed using a Vevo 770 (VisualSonics, Toronto, ON, Canada) with a linear 30-MHz probe (RMV 707B) as previously described (Yuan et al., 2010). For invasive hemodynamics, a 1.4 French catheter (Millar Instruments, Houston, TX) was inserted through the right carotid artery and then advanced into the left ventricle to record pressure and left ventricular function as previously reported (Xu et al., 2009).

Histopathology. The hearts from mice were fixed with 4% paraformaldehyde and then routinely dehydrated and embedded in blocks of paraffin wax and cross-sectioned at a thickness of 6 μm . Collagen accumulation in heart tissues underwent morphometric analysis and was assayed by Masson trichrome and Picrosirius red staining as previously described (Xu et al., 2009).

Real-Time Reverse-Transcription Polymerase Chain Reaction. Total RNA from infarcted and noninfarcted hearts was extracted using an RNeasy kit (Qiagen, Redwood City, CA) following the manufacturer's instructions, and the concentration of RNA was measured by nanodrop; 0.5 μg of each sample was applied for reverse transcription. Taqman universal PCR Master Mix and probes were used for real-time polymerase chain reaction.

Statistical Analysis. All data were expressed as means \pm S.E.M. Statistical differences were determined using two-way analysis of variance or two-tailed Student's t test as appropriate. A P value less than 0.05 was considered a significant difference.

Results

Myeloid mPges-1 Deletion Improved Post-MI Survival with Little Effect on Cardiac Function. To study the effects of myeloid mPges-1 deletion on cardiac response to myocardial infarction, Mac-mPges-1-WT or -KO male mice were subjected to coronary artery ligation, and the cardiac function was assessed by echocardiography before and 7 and 28 days after the surgery. Invasive hemodynamics was performed at the end of the experiment. Although the cardiac function was clearly impaired upon the ligation at 7 and 28 days postsurgery, no significant difference was observed between the WT and KO group for either the left ventricular systolic function (reflected by ejection fraction, fractional shortness, end systolic volume, and $+dP/dt$) or diastolic function (reflected by end diastolic volume, $-dP/dt$, and Tau) (Fig. 1, A and B; Table 1). However, the survival rate was significantly improved in the KO groups, with 9 deaths out of 26 mice in the WT mice and only 2 deaths of 24 in the KOs (Fig. 1C).

Post-MI Cardiac Hypertrophy and Fibrosis Were Not Affected by Myeloid mPges-1 Deletion. Masson trichrome and Picrosirius red staining showed no obvious difference between the WT and KO groups for the extracellular matrix deposition, which is a feature of post-MI ventricular remodeling (Fig. 2, A and B). We also compared the mRNA level for several

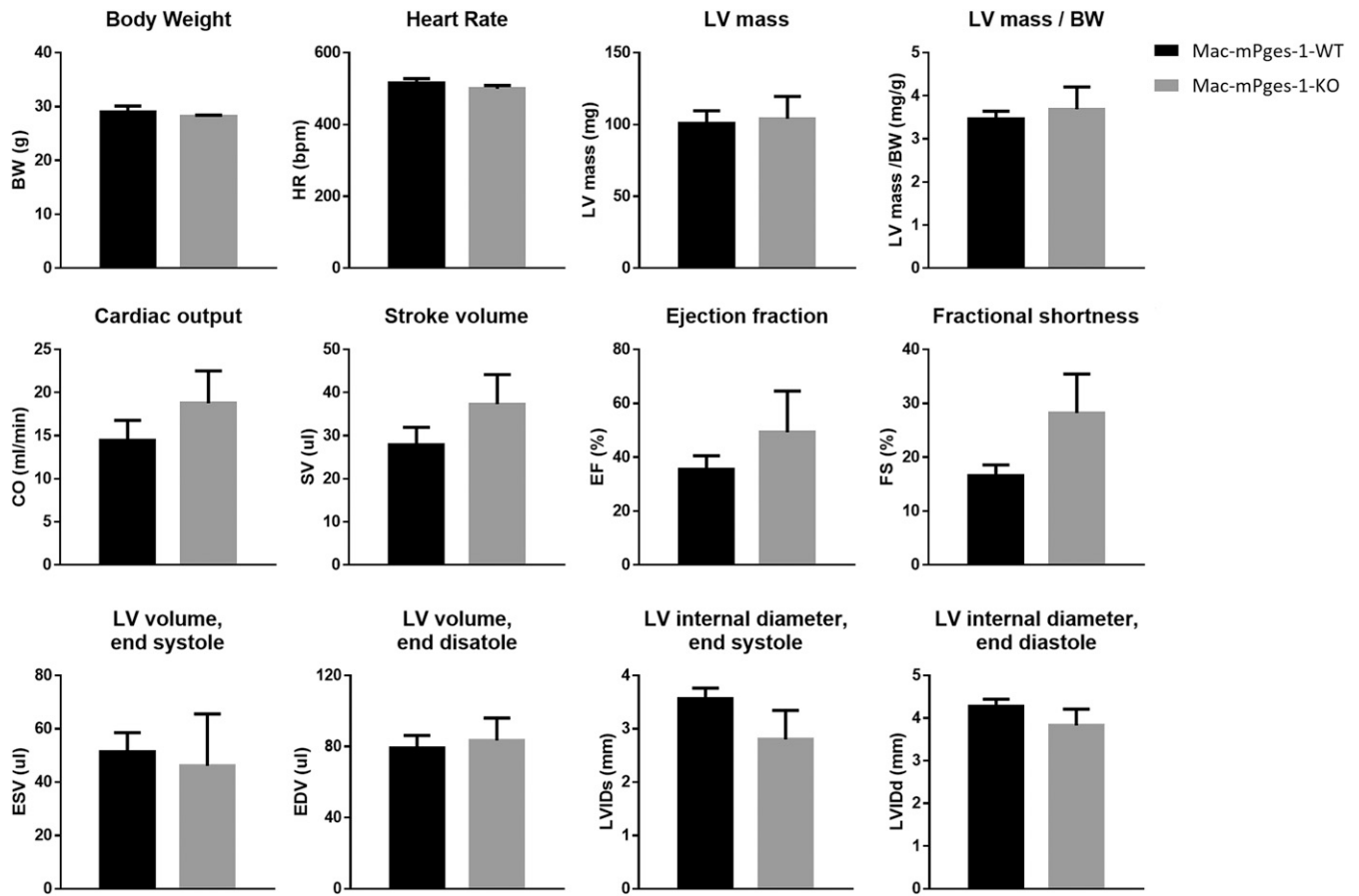


Fig. 3. Echocardiographic analysis of cardiac function in myeloid mPges-1 KO mice 3 days post-MI. BW, body weight; CO, cardiac output; EDV, left ventricular (LV) end-diastolic volume; EF, ejection fraction; ESV, LV end-systolic volume; FS, fractional shortness; HR, heart rate; LV mass/BW, ratio of left ventricular mass to body weight; LVIDd, LV diastolic internal dimensions; LVIDs, LV systolic internal dimensions; SV, stroke volume. $n = 3$ mice/group.

cardiac hypertrophy and fibrosis markers in both noninfarcted and infarcted heart zones. Irrespective of genotype, the infarcted heart showed markedly increased expression of both fibrosis-related (collagen synthases, transforming growth factor β , connective tissue growth factor) and hypertrophy-related genes (atria natriuretic peptide, brain natriuretic peptide, and β -major histocompatibility complex) (Fig. 2, C and D).

Inflammation and Apoptosis Were Not Affected by Myeloid mPges-1 Deletion. Inflammation and myocyte apoptosis soon after experimental MI may cause fibrosis and lead to progressive impairment of cardiac function. To determine whether mPges-1 deletion in myeloid cells might influence these processes, Mac-mPges-1-WT and -KO mice were subjected to acute coronary artery ligation, and heart function was assessed 3 days after. Similar to 7 or 28 days postinfarction, left ventricular function showed no significant difference between the two groups 3 days after the occlusion (Fig. 3). Gene expression relevant to both inflammation and apoptosis was also uninfluenced by genotype (Fig. 4).

Global mPges-1 Deletion Did Not Worsen Post-MI Cardiac Dysfunction. In addition to conditional myeloid cell deletion, we also studied the contribution of global mPges-1 deletion to post-MI remodeling. As shown in Fig. 5 and Table 2, left ventricular function, hypertrophy, and fibrosis were all unaltered in the global mPges-1 knockouts compared with controls.

Discussion

Both the cardiovascular adverse effects of nonsteroidal anti-inflammatory drugs and the opioid crisis have focused interest on mPGES-1, the dominant source of PGE₂ biosynthesis downstream of COX-2, as an analgesic and anti-inflammatory drug target (Kamei et al., 2004; Wang et al., 2008b; Koeberle and Werz, 2015). Compared with disruption of the COX-2/PGI₂ signaling pathway, deletion of mPges-1 is less likely to predispose to thrombogenesis, hypertension (Cheng et al., 2006), atherogenesis (Wang et al., 2006), a proliferative response to vascular injury (Wang et al., 2011), or aortic aneurysm formation (Wang et al., 2008a) in mice. This altered profile reflects, at least in part, the differential impact of the two strategies on biosynthesis of PGI₂; this is enhanced by mPges-1 deletion or blockade in mice and humans due to increased utilization of the mPGES-1 substrate, prostaglandin H₂, by PGI₂ synthase (Tang et al., 2016). Specific inhibitors of mPGES-1 have been under development (Koeberle et al., 2016; Di Micco et al., 2018; Ding et al., 2018), and the clinical pharmacology of several mPGES-1 inhibitors has been described (Jin et al., 2016). However, progress in bringing these drugs to the market is slow. Factors that have complicated the development of mPGES-1 inhibitors include off-target hepatotoxicity of some compounds (Jin et al., 2016) and the theoretical possibility that augmented PGI₂ formation may attenuate cardiovascular risk but also restrain analgesic efficacy in some

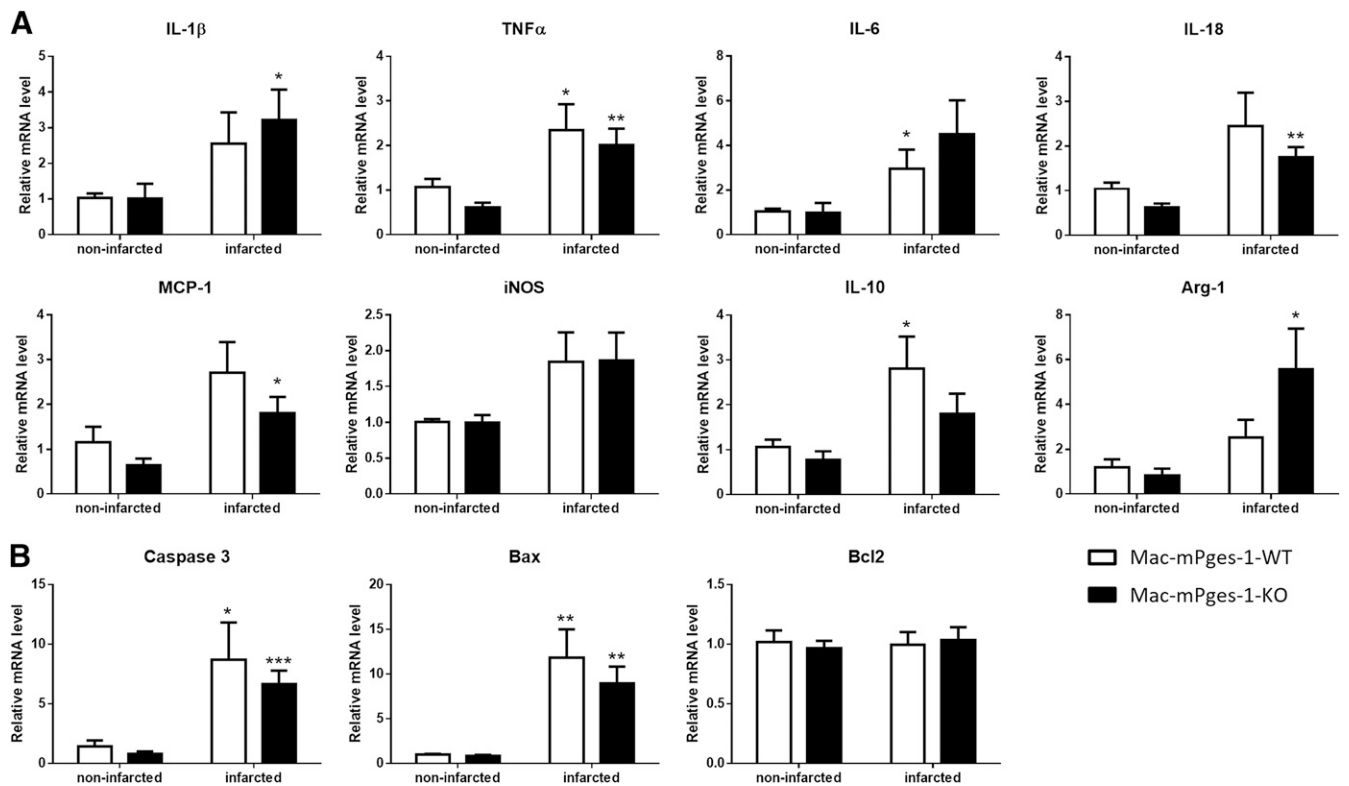


Fig. 4. Effect of myeloid mPges-1 deletion on post-MI inflammation and apoptosis. (A) Real-time polymerase chain reaction (PCR) analysis of the expression of inflammation-related genes in the hearts from mice 3 day post-MI. (B) Real-time PCR analysis of the expression of apoptosis-related genes in the hearts from mice 3 day post-MI. $n = 4$ to 5. * $P < 0.05$; ** $P < 0.01$; *** $P < 0.001$, noninfarcted vs. infarcted heart. IL, interleukin; iNOS, inducible Nitric Oxide Synthase; TNF α , tumor necrosis factor α .

settings (Pulichino et al., 2006). More recently, the opioid crisis has highlighted the limited number of analgesic options and has reinvigorated interest in inhibitors of mPGES-1.

Interestingly, deletion of mPges-1 in myeloid cells, within which the enzyme is most abundantly expressed in macrophages, attenuates the vascular proliferative response to injury and mitigates high-fat diet-induced atherosclerosis while conserving

the efficacy of nonsteroidal anti-inflammatory drugs in models of analgesia; by contrast, deletion of mPges-1 in vascular cells enhances the response to vascular injury (Chen, 2013; Chen et al., 2013, 2014). These observations have prompted us to pursue the possibility that targeting mPGES-1 selectively in activated macrophages might further improve the therapeutic index of mPGES-1 inhibitors.

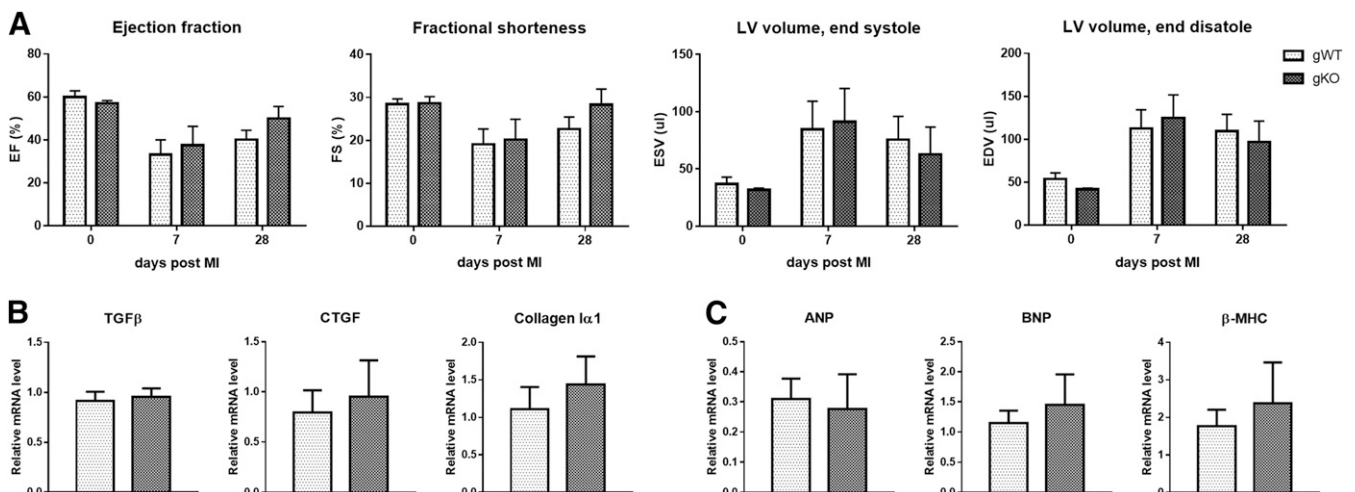


Fig. 5. Effect of global mPges-1 deletion on post-MI heart remodeling. (A) mPges-1 global KO and the control mice were subjected to coronary artery ligation, and heart function was assessed by echocardiography before and 7 and 28 days after the ligation. EDV, left ventricular (LV) end-diastolic volume; EF, ejection fraction; ESV, LV end-systolic volume; FS, fractional shortness; gKO, global mPges-1 KO; gWT, global mPges-1 WT. $n = 4$ –14 mice/group. (B) Real-time polymerase chain reaction (PCR) analysis of the expression of fibrosis-related genes in the hearts from mice 28 days post-MI. $n = 6$ –8. ANP, atria natriuretic peptide; BNP, brain natriuretic peptide; MHC, major histocompatibility complex; TGF, transforming growth factor. (C) Real-time PCR analysis of the expression of cardiac hypertrophy-related genes in the hearts from mice 28 days post-MI. $n = 6$ –8.

TABLE 2
Echocardiographic analysis of cardiac function in global mPges-1 KO mice

	Days after Coronary Ligation					
	0		7		28	
	gWT (n = 4)	gKO (n = 4)	gWT (n = 8)	gKO (n = 7)	gWT (n = 14)	gKO (n = 12)
Body weight (g)	28.73 ± 1.37	26.38 ± 1.25	24.28 ± 3.21	25.97 ± 3.58	25.13 ± .08	26.90 ± 2.29
LV mass (mg)	92.78 ± 9.89	82.71 ± 1058	90.88 ± 15.79	91.19 ± 16.42	86.35 ± 16.32	84.05 ± 19.79
LV mass/BW (mg/g)	3.24 ± 0.40	3.13 ± 0.30	3.76 ± 0.53	3.51 ± 0.45	3.49 ± 0.82	3.11 ± 0.63
Heart rate (bpm)	454.00 ± 49.77	401.75 ± 21.28	471.63 ± 62.80	481.43 ± 58.20	456.36 ± 64.58	460.17 ± 50.38
Cardiac output (ml/min)	23.91 ± 4.61	16.84 ± 0.82	12.70 ± 5.43	15.87 ± 4.98	15.34 ± 3.46	15.54 ± 2.33
Stroke volume (μl)	53.69 ± 14.46	41.97 ± 2.56	28.06 ± 13.25	33.38 ± 10.70	34.01 ± 7.78	34.26 ± 6.76
Ejection fraction (%)	59.91 ± 5.83	57.02 ± 2.49	33.14 ± 19.57	37.48 ± 23.40	40.07 ± 16.68	49.96 ± 19.42
Fractional shortness (%)	28.40 ± 2.48	28.60 ± 3.16	19.07 ± 10.14	20.18 ± 12.49	22.63 ± 10.52	28.27 ± 12.79
LV internal diameter, end systole (mm)	2.92 ± 0.43	2.83 ± 1.89	3.82 ± 1.29	4.06 ± 1.82	3.45 ± 1.51	3.08 ± 1.72
LV internal diameter, end diastole (mm)	4.07 ± 0.50	3.97 ± 0.11	4.63 ± 1.04	4.89 ± 1.52	4.32 ± 1.22	4.08 ± 1.40

BW, body weight; gKO, global mPges-1 KO; gWT, global mPges-1 WT; LV, left ventricular.

However, despite the relatively benign preclinical cardiovascular profile of targeting mPGES-1, doubts have been raised about the safety of this strategy in the setting of acute myocardial infarction. Unlike COX-2 inhibition, Wu et al. (2009a,b) reported that deletion of mPges-1 did not increase ischemic myocardial injury or death after coronary occlusion in mice. However, in a model of angiotensin II-mediated stress, Harding et al. (2011) found that mPges-1 deletion resulted in myocardial dysfunction, albeit without evidence of cardiomyocyte hypertrophy or fibrosis. Finally, Degousee et al. (2008, 2012) reported a reduction in survival and impaired cardiac remodeling after experimental MI in mice subjected to either global or myeloid cell deletion of mPges-1, the latter by bone marrow transfer in irradiated mice. Unexpectedly, they observed enhanced inflammation and higher PGE₂ in the infarct area in the myeloid cell mPges-1-deficient mice (Degousee et al., 2012).

Here, we generated mice lacking mPges-1 in myeloid cells by crossing mPges-1 floxed mice with LysMCre mice. As we previously reported, the dominant consequence of the enzyme deletion is to render macrophages deficient in mPges-1 (Chen et al., 2013). Here, by contrast, we found that post-MI survival was improved, and we did not observe any alteration in left ventricular function or postinfarction remodeling by genotype. Similarly, we failed to observe any detectable adverse influence on post-MI remodeling after mPges-1 was depleted globally. Several differences may explain this discrepancy from the reports of Degousee et al. (2008, 2012), including the cells deficient in mPges-1 (myeloid cells vs. bone marrow-derived leukocytes), the genetic background of the mice used in the two studies (C57BL/6 vs. DBA/11acJ), the surgical approaches to coronary artery ligation (nonthoracotomy vs. ventilated thoracotomy), and possibly the sex of the mice studied (males vs. female recipients for the bone marrow transplantation).

So far, many strategies for targeting disease-relevant macrophages have been developed. These include liposome-encapsulated drug delivery (Ahsan et al., 2002; Ergen et al., 2017); glucan particle-based delivery of small interfering RNA, protein, or small molecules to phagocytic cells (Aouadi et al., 2009; Tesz et al., 2011); nanotherapeutic delivery of high-density lipoprotein nanoparticle to atherosclerotic plaque macrophages (Duivenvoorden et al., 2014); and folate receptor-mediated therapeutic intervention (Xia et al., 2009; Ayala-López et al., 2010). Thus, many options can be explored

to target specifically inflammatory macrophages with inhibitors of mPGES-1.

Taken together, our findings predict a beneficial cardiovascular impact of mPGES-1 inhibition, even in the setting of myocardial infarction. However, given the conflicting results from distinct approaches to addressing this question in mice, further modeling with macrophage-directed inhibitors must occur before proceeding with their clinical development.

Acknowledgments

We acknowledge technical assistance from Weili Yan, Qiaoling Li, Xiangbo An, and Lei Qian.

Authorship Contributions

Participated in research design: Chen, Yang, M. Wang, FitzGerald.
Conducted experiments: Chen, Yang, Jiang, Tang, T. Wang, Wan.
Performed data analysis: Chen, Yang, Jiang.
Wrote or contributed to the writing of the manuscript: Chen, Yang, FitzGerald.

References

- Ahsan F, Rivas IP, Khan MA, and Torres Suarez AI (2002) Targeting to macrophages: role of physicochemical properties of particulate carriers-liposomes and microspheres--on the phagocytosis by macrophages. *J Control Release* **79**: 29–40.
- Aouadi M, Tesz GJ, Nicoloro SM, Wang M, Chouinard M, Soto E, Ostroff GR, and Czech MP (2009) Orally delivered siRNA targeting macrophage Map4k4 suppresses systemic inflammation. *Nature* **458**:1180–1184.
- Ayala-López W, Xia W, Varghese B, and Low PS (2010) Imaging of atherosclerosis in apolipoprotein e knockout mice: targeting of a folate-conjugated radiopharmaceutical to activated macrophages. *J Nucl Med* **51**:768–774.
- Chen L (2013) Macrophage prostaglandin E2 mediates inflammatory pain in peripheral tissues. *J Pain* **14**:S72.
- Chen L, Yang G, Monslow J, Todd L, Cormode DP, Tang J, Grant GR, DeLong JH, Tang SY, Lawson JA, et al. (2014) Myeloid cell microsomal prostaglandin E synthase-1 fosters atherogenesis in mice. *Proc Natl Acad Sci USA* **111**: 6828–6833.
- Chen L, Yang G, Xu X, Grant G, Lawson JA, Bohlooly-Y M, and FitzGerald GA (2013) Cell selective cardiovascular biology of microsomal prostaglandin E synthase-1. *Circulation* **127**:233–243.
- Cheng Y, Wang M, Yu Y, Lawson J, Funk CD, and FitzGerald GA (2006) Cyclooxygenases, microsomal prostaglandin E synthase-1, and cardiovascular function. *J Clin Invest* **116**: 1391–1399.
- Degousee N, Fazel S, Angoulvant D, Stefanski E, Pawelzik SC, Korotkova M, Arab S, Liu P, Lindsay TF, Zhuo S, et al. (2008) Microsomal prostaglandin E2 synthase-1 deletion leads to adverse left ventricular remodeling after myocardial infarction. *Circulation* **117**:1701–1710.
- Degousee N, Simpson J, Fazel S, Scholich K, Angoulvant D, Angioni C, Schmidt H, Korotkova M, Stefanski E, Wang XH, et al. (2012) Lack of microsomal prostaglandin E(2) synthase-1 in bone marrow-derived myeloid cells impairs left ventricular function and increases mortality after acute myocardial infarction. *Circulation* **125**:2904–2913.
- Di Micco S, Terracciano S, Cantone V, Fischer K, Koeberle A, Foglia A, Riccio R, Werz O, Bruno I, and Bifulco G (2018) Discovery of new potent molecular entities able to inhibit mPGES-1. *Eur J Med Chem* **143**:1419–1427.

- Ding K, Zhou Z, Zhou S, Yuan Y, Kim K, Zhang T, Zheng X, Zheng F, and Zhan CG (2018) Design, synthesis, and discovery of 5-((1,3-diphenyl-1H-pyrazol-4-yl)methylene)pyrimidine-2,4,6-(1H,3H,5H)-triones and related derivatives as novel inhibitors of mPGES-1. *Bioorg Med Chem Lett* **28**:858–862.
- Duivenvoorden R, Tang J, Cormode DP, Mieszawska AJ, Izquierdo-Garcia D, Ozcan C, Otten MJ, Zaidi N, Lobatto ME, van Rijs SM, et al. (2014) A statin-loaded reconstituted high-density lipoprotein nanoparticle inhibits atherosclerotic plaque inflammation [published correction appears in *Nat Commun* (2014) 5:3531]. *Nat Commun* **5**:3065.
- Ergen C, Heymann F, Al Rawashdeh W, Gremse F, Bartneck M, Panzer U, Pola R, Pechar M, Storm G, Mohr N, et al. (2017) Targeting distinct myeloid cell populations in vivo using polymers, liposomes and microbubbles. *Biomaterials* **114**:106–120.
- Friesen RW and Mancini JA (2008) Microsomal prostaglandin E2 synthase-1 (mPGES-1): a novel anti-inflammatory therapeutic target. *J Med Chem* **51**:4059–4067.
- Gao E, Lei YH, Shang X, Huang ZM, Zuo L, Boucher M, Fan Q, Chuprun JK, Ma XL, and Koch WJ (2010) A novel and efficient model of coronary artery ligation and myocardial infarction in the mouse. *Circ Res* **107**:1445–1453.
- Grosser T, Ricciotti E, and FitzGerald GA (2017a) The cardiovascular pharmacology of nonsteroidal anti-inflammatory drugs. *Trends Pharmacol Sci* **38**:733–748.
- Grosser T, Theken KN, and FitzGerald GA (2017b) Cyclooxygenase inhibition: pain, inflammation, and the cardiovascular system. *Clin Pharmacol Ther* **102**:611–622.
- Harding P, Yang XP, He Q, and Lapointe MC (2011) Lack of microsomal prostaglandin E synthase-1 reduces cardiac function following angiotensin II infusion. *Am J Physiol Heart Circ Physiol* **300**:H1053–H1061.
- Jin Y, Smith CL, Hu L, Campanale KM, Stoltz R, Huffman LG Jr, McNearney TA, Yang XY, Ackermann BL, Dean R, et al. (2016) Pharmacodynamic comparison of LY3023703, a novel microsomal prostaglandin E synthase 1 inhibitor, with celecoxib. *Clin Pharmacol Ther* **99**:274–284.
- Kamei D, Yamakawa K, Takegoshi Y, Mikami-Nakanishi M, Nakatani Y, Oh-Ishi S, Yasui H, Azuma Y, Hirasawa N, Ohuchi K, et al. (2004) Reduced pain hypersensitivity and inflammation in mice lacking microsomal prostaglandin e synthase-1. *J Biol Chem* **279**:33684–33695.
- Koerberle A, Laufer SA, and Werz O (2016) Design and development of microsomal prostaglandin E2 synthase-1 inhibitors: challenges and future directions. *J Med Chem* **59**:5970–5986.
- Koerberle A and Werz O (2015) Perspective of microsomal prostaglandin E2 synthase-1 as drug target in inflammation-related disorders. *Biochem Pharmacol* **98**:1–15.
- Pulichino AM, Rowland S, Wu T, Clark P, Xu D, Mathieu MC, Riendeau D, and Audoly LP (2006) Prostacyclin antagonism reduces pain and inflammation in rodent models of hyperalgesia and chronic arthritis. *J Pharmacol Exp Ther* **319**:1043–1050.
- Tang SY, Monslow J, R Grant G, Todd L, Pawelzik SC, Chen L, Lawson J, Puré E, and FitzGerald GA (2016) Cardiovascular consequences of prostanoid I receptor deletion in microsomal prostaglandin E synthase-1-deficient hyperlipidemic mice. *Circulation* **134**:328–338.
- Tez GJ, Aouadi M, Prot M, Nicoloso SM, Boutet E, Amano SU, Goller A, Wang M, Guo CA, Salomon WE, et al. (2011) Glucan particles for selective delivery of siRNA to phagocytic cells in mice. *Biochem J* **436**:351–362.
- Wang M and FitzGerald GA (2010) Cardiovascular biology of microsomal prostaglandin E synthase-1. *Trends Cardiovasc Med* **20**:189–195.
- Wang M, Ihida-Stansbury K, Kothapalli D, Tamby MC, Yu Z, Chen L, Grant G, Cheng Y, Lawson JA, Assoian RK, et al. (2011) Microsomal prostaglandin e2 synthase-1 modulates the response to vascular injury. *Circulation* **123**:631–639.
- Wang M, Lee E, Song W, Ricciotti E, Rader DJ, Lawson JA, Puré E, and FitzGerald GA (2008a) Microsomal prostaglandin E synthase-1 deletion suppresses oxidative stress and angiotensin II-induced abdominal aortic aneurysm formation. *Circulation* **117**:1302–1309.
- Wang M, Song WL, Cheng Y, and FitzGerald GA (2008b) Microsomal prostaglandin E synthase-1 inhibition in cardiovascular inflammatory disease. *J Intern Med* **263**:500–505.
- Wang M, Zukas AM, Hui Y, Ricciotti E, Puré E, and FitzGerald GA (2006) Deletion of microsomal prostaglandin E synthase-1 augments prostacyclin and retards atherogenesis. *Proc Natl Acad Sci USA* **103**:14507–14512.
- Wu D, Mennerich D, Arndt K, Sugiyama K, Ozaki N, Schwarz K, Wei J, Wu H, Bishopric NH, and Doods H (2009a) Comparison of microsomal prostaglandin E synthase-1 deletion and COX-2 inhibition in acute cardiac ischemia in mice. *Prostaglandins Other Lipid Mediat* **90**:21–25.
- Wu D, Mennerich D, Arndt K, Sugiyama K, Ozaki N, Schwarz K, Wei J, Wu H, Bishopric NH, and Doods H (2009b) The effects of microsomal prostaglandin E synthase-1 deletion in acute cardiac ischemia in mice. *Prostaglandins Leukot Essent Fatty Acids* **81**:31–33.
- Xia W, Hilgenbrink AR, Matteson EL, Lockwood MB, Cheng JX, and Low PS (2009) A functional folate receptor is induced during macrophage activation and can be used to target drugs to activated macrophages. *Blood* **113**:438–446.
- Xu J, Ismat FA, Wang T, Lu MM, Antonucci N, and Epstein JA (2009) Cardiomyocyte-specific loss of neurofibromin promotes cardiac hypertrophy and dysfunction. *Circ Res* **105**:304–311.
- Yu Y, Ricciotti E, Scalia R, Tang SY, Grant G, Yu Z, Landesberg G, Crichton I, Wu W, Puré E, et al. (2012) Vascular COX-2 modulates blood pressure and thrombosis in mice. *Sci Transl Med* **4**:132ra54.
- Yuan L, Wang T, Liu F, Cohen ED, and Patel VV (2010) An evaluation of transmitral and pulmonary venous Doppler indices for assessing murine left ventricular diastolic function. *J Am Soc Echocardiogr* **23**:887–897.

Address correspondence to: Dr. Garret A. FitzGerald, Institute for Translational Medicine and Therapeutics, Smilow Center for Translational Research, West Pavilion, 10th Floor, Room 116, 3400 Civic Center Boulevard, Building 421, Philadelphia, PA 19104-5158. E-mail: garret@upenn.edu; or Dr. Lihong Chen, Advanced Institute for Medical Sciences, Dalian Medical University, Dalian, Liaoning, China 116044. E-mail: lihong@dmu.edu.cn